



Research article

Eco-friendly approach for the fabrication of bio copper based superhydrophobic coating on steel metal and its corrosion resistance evaluation

R.S. Almufarj^a, M. Saadawy^b, M.E. Mohamed^{b,c,*}^a Department of Chemistry, College of Science, Princess Nourah bint Abdulrahman University, P.O. Box 84428, Riyadh 11671, Saudi Arabia^b Chemistry Department, Faculty of Science, Alexandria University, Alexandria, Egypt^c Faculty of Advanced Basic Sciences, Alamein International University, Alamein City, Matrouh Governorate, Egypt

ARTICLE INFO

Keywords:

Superhydrophobic coating
Steel
Corrosion resistance
Bio copper
Sustainability

ABSTRACT

This study presents an eco-friendly approach for constructing superhydrophobic (S.H.) coatings on steel surfaces. The bio Cu nanoparticles are synthesized using a biogenic process. Two types of coatings, Ni-S.A and Ni-bio Cu-S.A, were developed and characterized. The EDX results confirm the successful fabrication of two distinct coatings on the steel substrate: one involving the modification of nickel with stearic acid, Ni-S.A, and the other involving the modification of nickel with both bio-Cu and stearic acid, Ni-bio Cu-S.A. The SEM results revealed that the S.H. coats exhibit circular microstructures which contribute to the surface roughness. The contact angles of water droplets on the Ni-S.A and Ni-bio Cu-S.A coatings were measured at $158^\circ \pm 0.9^\circ$ and $162^\circ \pm 1.1^\circ$, respectively. Chemical stability tests demonstrated that the Ni-S.A coating maintains its S.H. behaviour in a pH range of 3–11, whereas the Ni-bio Cu-S.A coating exhibits excellent chemical stability in a broader range of pH (1–13). The coating's mechanical stability was evaluated through abrasion tests. The Ni-S.A coating retained its S.H. properties even after an abrasion length equal 1100 mm, while the Ni-bio Cu-S.A coating maintained its S.H. behaviour till an abrasion length equal 1900 mm. The corrosion behavior and protective properties of the S.H. coatings were studied via electrochemical impedance spectroscopy (EIS) and potentiodynamic polarization (PDP) techniques. The PDP and EIS findings demonstrated that both Ni-S.A and Ni-bio Cu-S.A coatings significantly reduced the corrosion rate compared to uncoated steel.

1. Introduction

Superhydrophobic (S.H.) surfaces, have a water contact angle higher than 150° and exceptional water resistance, have garnered significant interest for their diverse applications in fields such as drag reduction, sensors, anti-icing, self-cleaning, antifouling, oil-water separation, and corrosion resistance [1–7]. Various techniques, including sol-gel, electrospinning, anodization, spraying, electrodeposition, 3D printing, chemical etching, and chemical vapor deposition, have been employed to achieve S.H. surfaces [8–14]. Electrodeposition, in particular, stands out as a simple, cost-effective, and flexible method for producing artificial S.H. surfaces [14]. Despite its advantages, the chemical and mechanical stability limitations, as well as the brittleness of microscopic nanostructures, have hindered the widespread commercialization of S.H. surfaces. To overcome these challenges, researchers have focused on enhancing the

* Corresponding author. Chemistry Department, Faculty of Science, Alexandria University, Alexandria, Egypt.
E-mail address: elshahatchemist93@gmail.com (M.E. Mohamed).

chemical stability and mechanical abrasion resistance of S.H. surfaces.

One key requirement for achieving S.H. surfaces is to increase surface roughness while simultaneously reducing surface energy [15]. In the past, perfluorinated compounds were commonly utilized to reduce surface energy due to their extremely low surface energy values [14]. However, these compounds were associated with toxicity and harmful environmental effects. Consequently, there is a growing need for eco-friendly techniques and materials to produce S.H. surfaces. Researchers have explored various nanomaterials, including metal-organic frameworks, carbon nanotubes, SiO₂, TiO₂, and ZnO to enhance surface roughness [7,16–18].

The synthesis of nanoparticles can be achieved through bottom-up (chemical and biological) and top-down (physical) methods [19]. However, chemical and physical procedures are often environmentally hazardous, toxic, and expensive. Various biotic resources such as microorganisms, fungi, algae, plants, and actinomycetes have been utilized in the eco-friendly synthesis of nanoparticles [20]. Plant extracts, in particular, have emerged as potential precursors for the eco-friendly manufacturing of nanomaterials. Active compounds present in plant extracts, including enzymes, carbohydrates, polyphenols, phenolics, and proteins, can act as stabilizers, reducing and capping agents for metal ions, facilitating the formation of metal nanoparticles [21].

Among the diverse range of nanoparticles, copper nanoparticles have gained more interest as their distinctive chemical and physical properties, make them suitable for numerous domestic and commercial applications. These applications include cosmetics, imaging, catalysis, medical and pharmaceutical purposes, environmental, and energy research applications. Copper nanoparticles find wide utility in the preparation of organic-inorganic nano-composites and as materials for gas sensors, and giant magneto-resistance. Furthermore, copper nanoparticles play a crucial role in medicine as antifungal agents, antibacterial agents, and antioxidants [22–24].

Steel is a widely used material in various industries due to its versatility, durability, and exceptional strength. It serves as a fundamental component in infrastructure, construction, transportation, manufacturing, and many other sectors [25,26]. However, steel is susceptible to corrosion when exposed to moisture, oxygen, and aggressive environments. Corrosion not only compromises the structural integrity of steel but also leads to significant economic losses due to repairs, replacements, and maintenance. Therefore, effective corrosion protection measures are crucial to extend the lifespan of steel structures, enhance their reliability, and minimize the financial and environmental impact of corrosion. By implementing corrosion protection techniques such as coatings, inhibitors, cathodic protection, and proper maintenance practices, the integrity and performance of steel can be preserved, ensuring its continued contribution to various industries.

The investigation into corrosion protection for metals and alloys has gained significant attention in recent years [27]. Various polymers, both thermoplastic and thermoset, including fluoropolymers, polypropylene, polyurethane, epoxy/silane, and poly-etherimide, have proven effective as coatings for corrosion prevention [28]. In their study, M. Kaseem and H. Choe explored the surface coatings characteristics of bioactive elements produced on Tie-6-Ale-4V alloy through plasma electrolytic oxidation (PEO). The incorporation of Mg and Zn into the surface was achieved by PEO treatment using electrolytes containing Zn²⁺ and Mg²⁺ ions at varying concentrations [29]. A.S. Gnedkov et al. introduced a self-healing PEO-based protective layer design of in-situ grown layered double hydroxides loaded with inhibitors on the MA8 magnesium alloy [30]. A novel approach has been suggested to create composite coatings that provide active corrosion protection for magnesium alloys. This method involves employing the Plasma Electrolytic Oxidation (PEO) technique and assessing the vulnerability of PEO layers to localized pitting formation using specialized electrochemical methods (SVET/SIET) [31]. A groundbreaking method was introduced by A. S. Gnedkov et al. to achieve enhanced corrosion protection for magnesium alloys using intelligent, environmentally friendly hybrid coatings containing inhibitors. This innovative approach involves elevating the corrosion resistance of magnesium and its alloys by creating self-healing hybrid coatings through plasma electrolytic oxidation (PEO) treatment. The process includes synthesizing a ceramic-like bioactive coating on the surface and subsequently infusing the resulting porous PEO layer with the corrosion inhibitor 8-hydroxyquinoline (8-HQ) and the bioresorbable polymer polycaprolactone (PCL) in various configurations, aiming to enhance protective properties [32]. A. S. Gnedkov et al. developed a new self-healing coating containing polycaprolactone to improve the corrosion resistance of magnesium and its alloys. This was achieved through plasma electrolytic oxidation (PEO) followed by treatment with an organic biocompatible corrosion inhibitor and a bioresorbable polymer, resulting in the formation of protective layers [33]. Furthermore, plasma electrolytic oxidation coatings exhibit substantial potential for surface alteration in Mg-based biodegradable constituents, allowing for wide adjustments in composition and properties to regulate degradation and attain biocompatibility [34].

The objective of this research is to fabricate a superhydrophobic coating on steel using bio-Cu. Two rough coatings of nickel, and nickel grafted with bio-Cu (Ni-bio Cu), were electrostatically deposited onto the steel surface. These coatings were then submerged in an ethanolic solution of stearic acid (S.A) to fabricate S.H. coating. To enhance the chemical and mechanical stability of the S.H. coatings, we innovatively employed bio Cu. To the best of our knowledge, this is the first report utilizing bio Cu as an additive to fabricate a S.H. coating on a steel substrate. Stearic acid, an eco-friendly substance and a cost-effective alternative to toxic fluorinated polymers was chosen as the low surface energy compound. The prepared S.H. coatings were evaluated for their wettability, chemical and mechanical stability, and corrosion resistance in a 1.0 M HCl solution. By addressing these research objectives, we aim to contribute to the development of durable, corrosion-resistant, and eco-friendly superhydrophobic coatings on steel, with potential applications in various industries and sectors.

2. Experimental

2.1. Materials

In this experimental study, a steel plate with dimensions of 2.0 cm × 1.0 cm x 0.1 cm was utilized. Analytical-grade chemicals including nickel sulfate (98.0 %), nickel chloride hexahydrate (99.0 %), copper sulfate pentahydrate (98.0 %), stearic acid (98.5 %),

boric acid (99.5 %), sodium hydroxide (97.0 %), hydrochloric acid (36.5-38.0%), sulfuric acid (97.0 %), and anhydrous ethanol (99.5 %), were employed.

2.2. Preparation of bio copper

To prepare the grape seed (G.S) powder, the grape seeds were carefully cleaned and dried at room conditions. Afterward, they were meticulously milled into a powder and then subjected to a drying process in an oven at 60 °C for 6 h. The G.S powder (10 g) was mixed with distilled water and refluxed for 1 h to obtain the G.S extract. The resulting solution was filtered, and the concentration of G.S extract was determined by evaporating 10 ml, weighing the residue, and calculating concentration in parts per million (ppm). A 10 mM solution of $\text{CuSO}_4 \cdot 5\text{H}_2\text{O}$ was prepared and added to the G.S extract to achieve a final concentration of 1 mM $\text{CuSO}_4 \cdot 5\text{H}_2\text{O}$ and 10 ppm G.S extract. The mixture was stirred on a magnetic stirrer for 5 h, resulting in the formation of dark brown copper nanoparticles (Cu NPs).

2.3. Construction of superhydrophobic coating

Before electrodeposition, the steel plate was polished via sandpaper of various grades, starting from a rough grade (150) and finishing with a smoother one (1000). The steel was then cleaned via its immersion in soapy water for 10 min, rinsed via distilled water, and submerged in 2.0 M sulfuric acid for 1 min. Following this preparation, the steel plate was placed in the electrodeposition bath. The coating process parameters, which involved depositing nickel (Ni) and an altered form of Ni using bio Cu (Ni-bio Cu), are mentioned in Table 1. The steel plate acted as the cathode and was positioned 2.0 cm away from the platinum anode. After the coatings were applied, the coated substrates were cleaned with distilled water and left to dry in air for 24 h. Subsequently, the coatings were altered by immersing them in an ethanolic solution of 10^{-2} M S.A for 15 min, washed with ethanol, and allowed to dry overnight. The coated steel plate with Ni altered by S.A (Ni-S.A) and the coated steel plate with Ni-bio Cu altered by S.A (Ni-bio Cu-S.A) were exposed to different characterization processes. Fig. 1 shows a scheme for the fabrication of the S.H. coated steel.

2.4. Coatings characterization

The morphology of the S.H. coatings was analyzed using a scanning electron microscope (SEM) (JSM-200 IT, JEOL). Elemental composition was examined using an energy-dispersive x-ray spectrometer (EDX JEM-2100 Japan). The water sliding angle (SA) and water contact angle (CA) were calculated by employing a 5 μL water droplet and an optical contact angle goniometer (model 190-F2, Ramehart CA instrument). The water contact angle and sliding angle readings were determined by averaging three measurements taken at various locations on the substrate.

2.5. Chemical stability

The S.H. coatings were immersed 1 h in various pH solutions ranging from 1.0 to 13, and the WCA and WSA were evaluated after each pH. Sodium hydroxide and sulfuric acid were used to alter the pH of the solutions. Based on the average of three tests performed on various substrates, the chemical stability data were calculated.

2.6. Mechanical abrasion

Two experiments were conducted to estimate the S.H. coating's mechanical properties: the abrasion test and the sand impact test. In the abrasion test, 6.0 kPa pressure was used while the S.H. coating was placed against SiC paper (600-grade). After each 100 mm of abrasion, the CA and SA are measured. In the sand impact test, 60 g of sand was fallen from a height of 600 mm onto the S.H. coated steel. The WCAs and WSAs were estimated after each 60 g of sand impact to assess the water superhydrophobicity of the material. The reported results are the average of three experiments conducted on various substrates.

2.7. Corrosion test

Electrochemical tests were done via a three-electrode cell and a Gamry PC14G300 Potentiostat/Galvanostat was used to assess the

Table 1
Various electrodeposition parameters for Ni-S.A and Ni- Bio-Cu-S.A coating on the steel surface.

Factor		Level	Level
(Nickel ions source)	$\text{NiCl}_2 \cdot 6\text{H}_2\text{O}$	40 gL^{-1}	40 gL^{-1}
	NiSO_4	176 gL^{-1}	176 gL^{-1}
(pH buffer)	H_3BO_3	60 gL^{-1}	60 gL^{-1}
Bio Cu		0.0 gL^{-1}	0.2 gL^{-1}
Electrodeposition time		6.0 min	6.0 min
Deposition potential		10.5 V	10.5 V

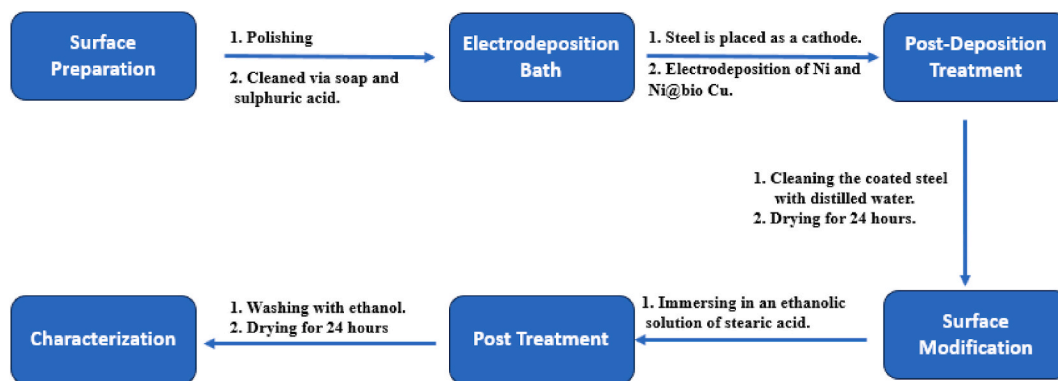


Fig. 1. A scheme for the fabrication of the S.H. coated steel.

electrochemical impedance spectroscopy (EIS) and the potentiodynamic polarization (PDP) curves. The counter electrode was a platinum rod, and a reference electrode was represented by an Ag/AgCl electrode. The working electrode was the steel sample, which was either uncoated or coated with S.H. films containing Ni-S.A or Ni-bio Cu-S.A. An epoxy layer was applied to the coated samples, leaving a 1 cm^2 area uncoated for exposure to the test solution. Before the electrochemical experiments, the steel samples were immersed in 1.0 M HCl for 15 min to reach the rest potential. The experimental setup of both EIS and PDP were like those reported previously [35]. The EIS measurements covered a frequency range of $0.01 \leq f \leq 1.0 \times 10^4$, and signal amplitude was set at 10 mV around the open circuit potential. The PDP measurements were conducted at a scan rate of 30 mV/min within a potential range of $\pm 300 \text{ mV}$ around the open circuit potential. We employed the Gamry software for PDP analysis to obtain the corrosion parameters. The experiments underwent a triple examination to ensure measurement precision, with the error staying within 2% .

3. Results and discussion

3.1. EDX results

The EDX technique is used to confirm the composition of the examined Bio Cu, steel coated with Ni-S.A, and steel coated with Ni-bio Cu-S.A. Fig. 2 illustrates the EDX spectra of Bio Cu, steel coated with Ni-S.A, and steel coated via Ni-bio Cu-S.A. The EDX micrograph of Bio Cu, Fig. 2a, reveals the presence of peaks corresponding to Cu NPs, indicating the successful synthesis of Bio Cu NPs. The EDX micrograph of steel coated with Ni-S.A, Fig. 2b, exhibits peaks corresponding to Fe, Ni, C, and O. These elements are expected as they are associated with the steel substrate and the Ni-S.A coating. The presence of Fe refers to the steel substrate, while Ni represents the Ni component of the coating. The peaks for C and O are likely associated with the organic stearic acid components in the coating material. In the EDX micrograph of steel coated with Ni-bio Cu-S.A, Fig. 2c, the same peaks observed in the steel coated with Ni-S.A are present. Additionally, there is an additional peak corresponding to bio Cu. This confirms the successful incorporation of bio Cu into the formed S.H. coating.

3.2. SEM and wettability

Fig. 3 displays the SEM micrographs of the coated steel using Ni-bio Cu-S.A and Ni-S.A. The discussion regarding the SEM results of the S.H. coated steel with Ni-bio Cu-S.A and Ni-S.A primarily revolves around the disparities in surface roughness and microstructure between the two coatings. Based on the SEM findings, it is observed that the coating formed with Ni-bio Cu-S.A, Fig. 3b, exhibits smaller circular microstructures in comparison with the coating formed with Ni-S.A, Fig. 3a. This discrepancy in microstructure size can be attributed to the inclusion of bio Cu in the Ni-bio Cu-S.A coating, which serves as a nucleation center during the electrodeposition process. The presence of bio Cu accelerates the nucleation process, favoring the formation of smaller structures rather than extensive crystal growth. This, in turn, results in increased surface roughness. The reduced microstructure size contributes to the S.H. characteristics of the coating. Smaller structures tend to enhance surface roughness, leading to a higher stability and water-repellent coating. Consequently, the S.H. characteristics of the coating are improved.

To evaluate the wettability of the Ni-S.A and Ni-bio Cu-S.A coatings, the WCA and WSA measurements were performed. The Ni-S.A coating exhibited a WCA of $158^\circ \pm 0.9^\circ$ and a WSA of $3^\circ \pm 0.1^\circ$. On the other hand, the Ni-bio Cu-S.A coating demonstrated a WCA of $162^\circ \pm 1.1^\circ$ and a WSA of $1^\circ \pm 0.1^\circ$. These results indicate that both coatings possess excellent S.H. properties.

3.3. Chemical stability

Chemical stability is a crucial condition for S.H. coatings to maintain their effectiveness over time, especially in harsh environments. The relationship between the solution pH and the WCAs and WSAs of water droplets on the S.H. coatings is illustrated in Fig. 4. The findings demonstrate that the Ni-S.A films, Fig. 4a, exhibit superhydrophobicity in a pH range of 3–11. Similarly, the Ni-bio Cu-S.A

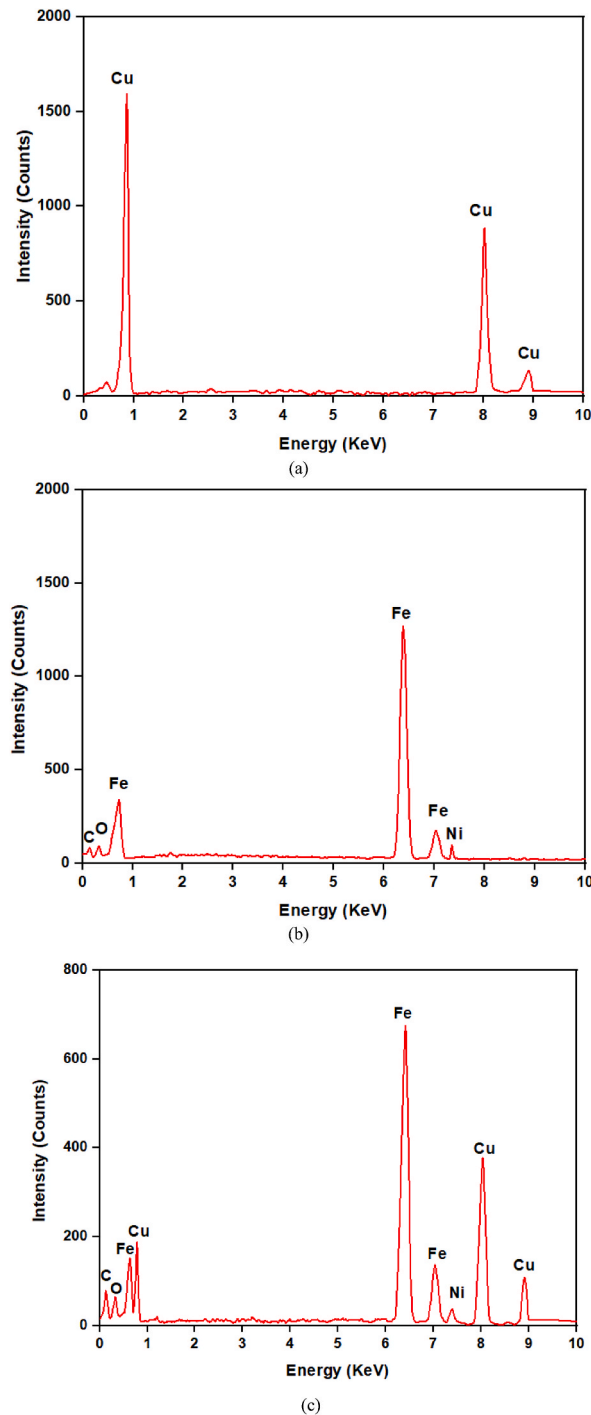


Fig. 2. EDX micrographs for a) bio Cu, and steel coated by b) Ni-S.A., and c) Ni-bio Cu-S.A.

films, Fig. 4b, exhibit superhydrophobicity in a broader pH range of 1–13. In both cases, the WCAs are consistently greater than 150° , indicating strong water repellency, while the WSAs remain lower than 10° , indicating excellent water sliding properties. These pH ranges highlight the robustness of the coatings in various alkaline and acidic environments.

Comparatively, the chemical stability of the S.H. coated steel with Ni-bio Cu-S.A is superior to that of the steel coated with Ni-S.A. The inclusion of bio Cu in the Ni-bio Cu-S.A coating not only enhances the superhydrophobicity of the coating but also provides an additional layer of protection. This added layer contributes to the improved chemical stability of the coating, making it more resistant to degradation and maintaining its S.H. properties over extended periods. Remarkably, the S.H. coated steel with Ni-bio Cu-S.A

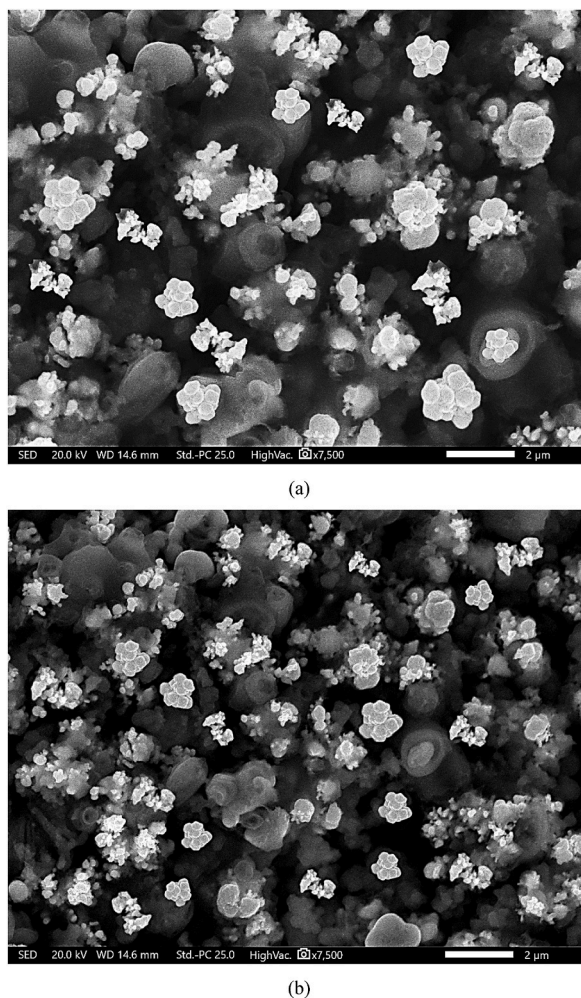


Fig. 3. SEM images of coated steel with a) Ni-S.A, and b) Ni-bio Cu-S.A.

exhibits superior chemical stability when compared to numerous reported values in the literature [36–39] [36–39] [36–39]. This indicates that the coating's performance surpasses existing studies, further emphasizing its effectiveness in harsh solution conditions and its potential for long-term applications. The coating's ability to withstand a wide pH range and outperform previous research findings highlights its potential for practical applications in corrosive or challenging environments.

3.4. Mechanical stability

Superhydrophobic (S.H.) surfaces, despite their advantageous properties, often suffer from reduced practical applications due to their mechanical fragility. In some cases, simply touching S.H. surfaces with a finger can cause them to lose their S.H. characteristics and become damaged [40]. To assess the resistance of the produced S.H. films to mechanical abrasion, abrasion, and sand impact tests were conducted. Fig. 5 illustrates the change in WCAs and WSAs of the fabricated S.H. films as a function of the length of abrasion. The Ni-S.A film, Fig. 5a, maintains its S.H. behaviour till a length of abrasion equals 1100 mm. In contrast, the Ni-bio Cu-S.A film, Fig. 5b, retains its S.H. properties even till a length of abrasion equals 1900 mm. Impressively, the S.H. coated steel with Ni-bio Cu-S.A exhibits superior abrasion resistance when compared to numerous reported values [25,41]. This indicates that the coating's ability to withstand mechanical abrasion surpasses previous studies, making it more durable and suitable for practical applications where mechanical stress is a concern. The enhanced mechanical abrasion resistance of the S.H. coated steel using Ni-bio Cu-S.A is due to the presence of the bio Cu layer. The bio Cu layer not only enhances the superhydrophobicity of the coating but also provides an additional protective barrier. This additional layer of protection contributes to the durability and abrasion resistance of the coating, allowing it to maintain its S.H. properties even under harsh mechanical conditions.

Furthermore, sand abrasion tests were conducted to determine the mechanical characteristics of the S.H. coatings, as shown in Fig. 6. The Ni-S.A film, Fig. 6a, retains its S.H. behaviours till 8 cycles of the sand impact, while the Ni-bio Cu-S.A film, Fig. 6b, maintains superhydrophobicity till 14 cycles of the sand impact. Notably, the Ni-bio Cu-S.A coating demonstrates sand impact

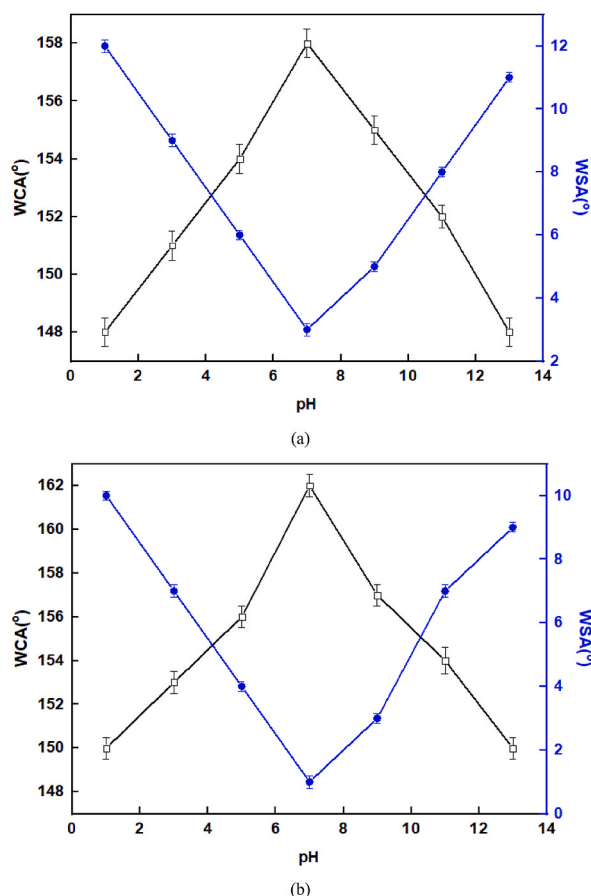


Fig. 4. The variation of the WCA and WSA of the S.H. coated steel via a) Ni-S.A, and b) Ni-bio Cu-S.A with the solution pH.

resistance that exceeds several reported values [38,42].

3.5. Corrosion measurements

3.5.1. PDP results

In addition to the microstructural, chemical stability, and mechanical properties of S.H. coatings, the corrosion characteristics of uncoated steel and S.H. coated steel using Ni-S.A and Ni-bio Cu-S.A have been investigated through the PDP technique. Fig. 7 presents the PDP plots of bare steel and S.H. coated steel in an aqueous solution of 1.0 M HCl. The PDP curves of uncoated steel in 1.0 M HCl show typical Tafel behavior indicating that the dissolution of steel takes place under the charge transfer process. However, in the presence of S.H. coatings, the anodic part of the graph may not exhibit Tafel behavior, unlike the blank. This observation suggests that the S.H. coatings have a significant impact on the anodic corrosion process. The absence of Tafel behavior in the anodic branch of the PDP graph can be attributed to the inhibiting effect of the S.H. coatings. These coatings create a physical barrier between the corrosive environment (1.0 M HCl) and the steel surface, reducing the availability of corrosive species and hindering the corrosion reaction. The S.H. coatings can alter the mass transport of reactants and products at the steel-coating interface, leading to a modified electrochemical behavior. This alteration in the anodic part of the graph could be due to a combination of factors such as reduced access of corrosive ions to the steel surface, changes in the kinetics of the corrosion reaction, or the creation of a protective film on the steel substrate. It's important to note that the cathodic part of the graph still exhibits Tafel behavior because the reduction reactions involved in corrosion are less affected by the presence of the S.H. coatings.

Table 2 provides the PDP parameters for uncoated steel and S.H. coated steel, including the protection efficiency (% η), corrosion potential (E_{corr}), and corrosion current density (i_{corr}). The % η value is determined using equation (1):

$$\% \eta = [(i_0 - i) / i_0] \times 100 \quad (1)$$

Where i and i_0 respectively, stand for the corrosion current densities of S.H. coated steel and uncoated steel. The i_{corr} value for steel coated with Ni-S.A is smaller than that of uncoated steel due to the S.H. properties of the coating. The presence of air trapped within the microstructures of the S.H. coating reduces the surface area available for contact between the solution and the steel, leading to a

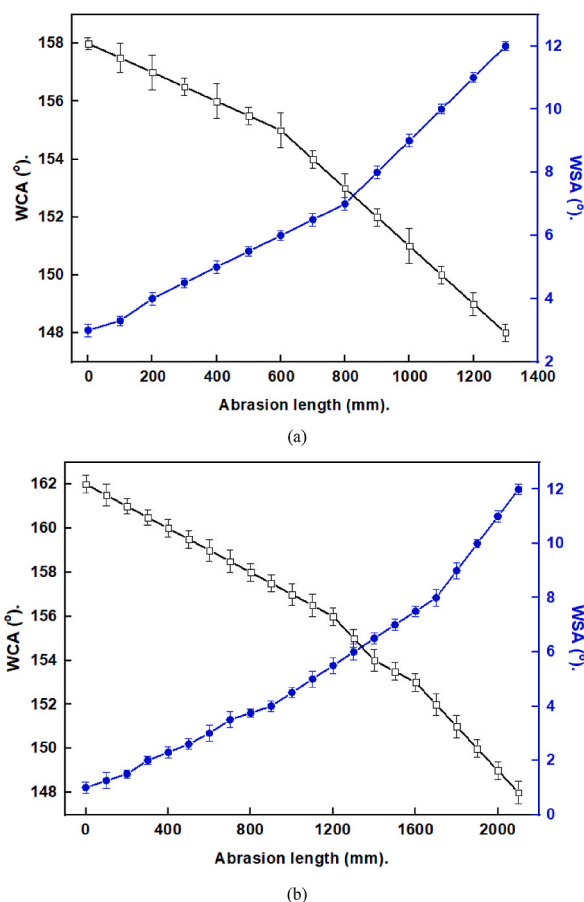


Fig. 5. The variation in WCAs and WSAs with the abrasion length for S.H. coated steel via a) Ni-S.A., and b) Ni-bio Cu-S.A.

faster decrease in the i_{corr} value. Furthermore, by incorporating bio Cu into the Ni-S.A. coating, the S.H. properties are enhanced, resulting in a higher reduction in the contact area between the medium and the steel. Consequently, the steel coated with Ni-bio Cu-S.A. exhibits a higher protection efficiency compared to the coated steel with Ni-S.A. These findings highlight the potential of S.H. coatings, particularly those with Ni-bio Cu-S.A., for corrosion protection applications in aggressive environments.

3.5.2. EIS results

Fig. 8 demonstrates the Nyquist plots and Bode plots comparing the corrosion characteristics of bare steel and S.H. coated steel in a 1.0 M HCl solution. The presence of a depressed capacitive semicircle in the Nyquist plots, Fig. 8a, at high frequencies, suggests that there is an interfacial charge transfer reaction. The capacitive semicircle size in the Nyquist plot is indicative of the corrosion resistance of the steel. A larger semicircle corresponds to a higher impedance, suggesting a greater resistance to charge transfer and, therefore, a lower corrosion rate. This implies that the steel is less sensitive to corrosion in the presence of the S.H. coatings. When the S.H. coatings are applied to the steel surface, they create a barrier between the corrosive environment and the steel substrate. This barrier reduces the exposure of the steel to the corrosive solution, leading to a decline in the corrosion rate. Consequently, the capacitive semicircle in the Nyquist plot becomes larger, indicating an increase in the impedance and enhanced corrosion resistance. The increase in the size of the capacitive semicircle can be due to the hindrance of the charge transfer reactions at the steel-coating interface. The S.H. coatings prevent the penetration of moisture and ions, reducing the availability of corrosive species and creating a more favorable environment for the creation of a protective layer on the steel substrate. This protective film acts as a physical and chemical barrier, further inhibiting the corrosion process. These results imply that the existence of a protective S.H. layer is what accounts for the increased charge transfer resistance of steel coated with Ni-SA. The steel coated with Ni-bio Cu-S.A. demonstrates the highest level of protection, as evidenced by the largest capacitive semicircle in the Nyquist plot. Bio-Cu is added to the Ni-coating to increase superhydrophobicity, which enables the Ni-bio Cu-coating to effectively stop the diffusion of corrosive species like Cl^- and H_2O into the steel. The superhydrophobic coating applied to the steel surface demonstrates enhanced impedance magnitudes at lower frequencies in the Bode plots when exposed to a 1.0 M HCl solution, as depicted in Fig. 8b. This observation affirms the superior protective properties of the manufactured superhydrophobic coating over bare steel. The phase angle plot in Fig. 8c reveals a distinct time constant at intermediate frequencies, indicating the presence of an electrical double layer. This time constant, occurring at moderate frequencies, is attributed

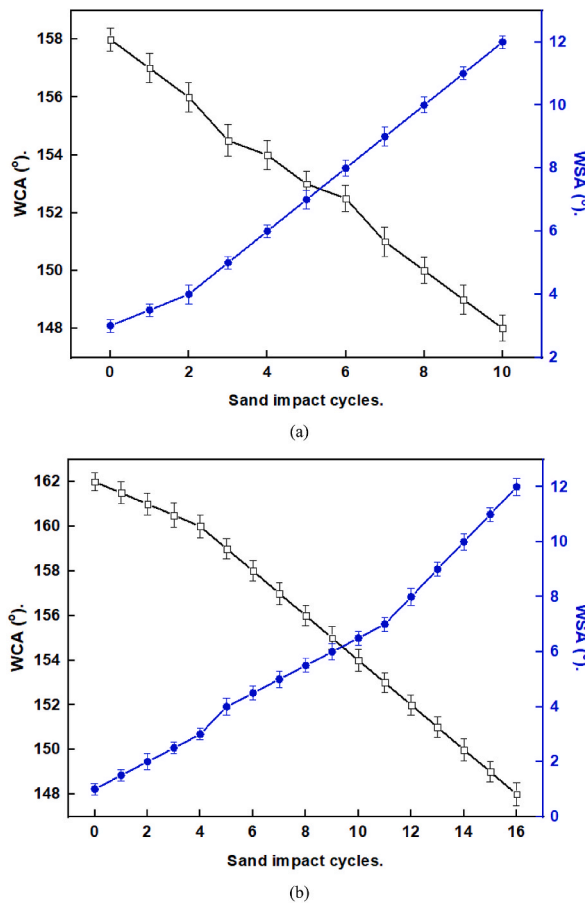


Fig. 6. The relation between the WCAs and WSAs of S.H. coated steel with a) Ni-S.A, and b) Ni-bio Cu-S.A with the sand impact cycles.

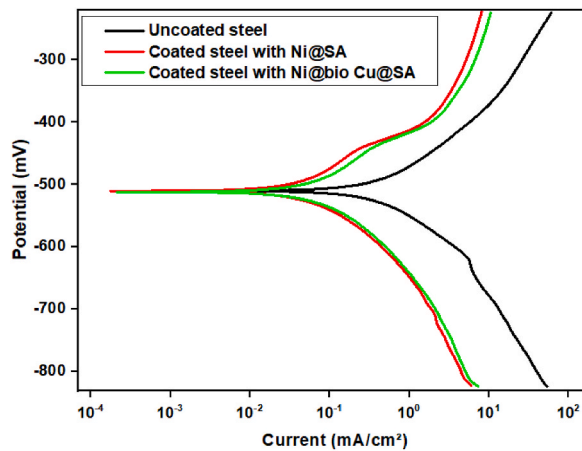


Fig. 7. The PDP plots of bare steel and S.H. coated steel.

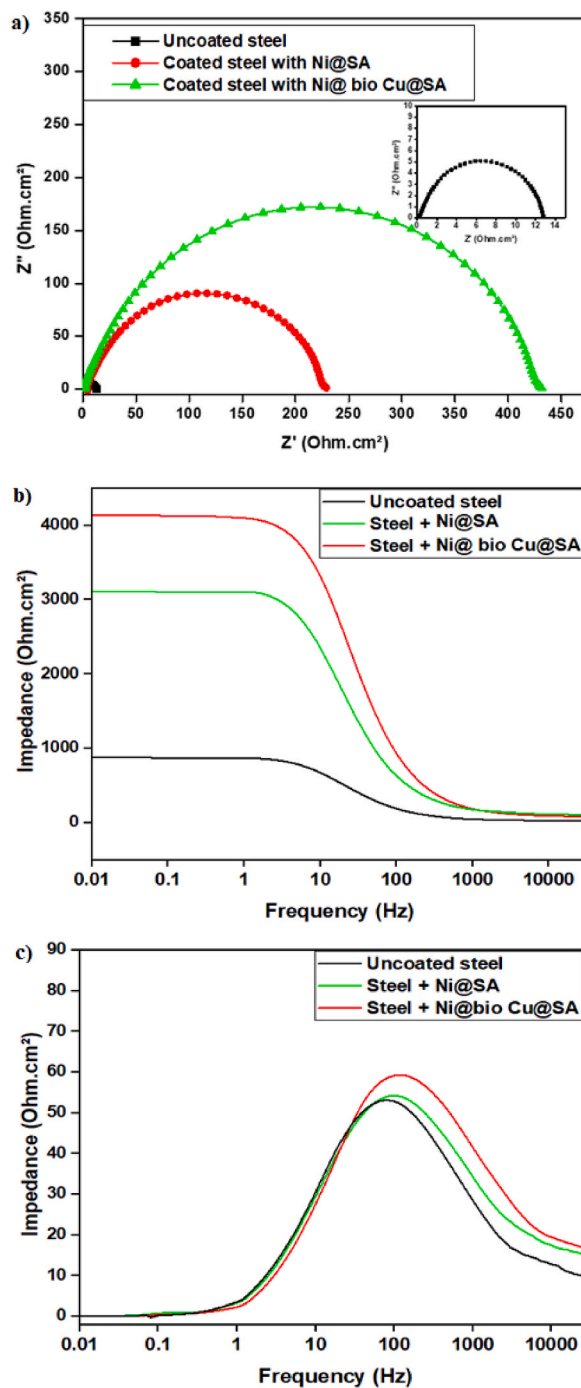
to the role of the electrical double layer in the corrosion protection mechanism. Overall, the Bode and phase angle plots collectively highlight the efficacy of the superhydrophobic coating in mitigating corrosion effects on the steel substrate [43,44].

To analyze the experimental results and calculate the impedance parameters, the equivalent circuit presented in Fig. 9 was employed, and the Zsimpwin program was used. The equivalent circuit consists of the charge transfer resistance (R_{ct}), the constant phase element (CPE), and solution resistance (R_s). Table 3 presents the EIS parameters for both uncoated steel and S.H. coated steel. The % η was calculated using equation (2):

Table 2

The PDP parameters for the uncoated and the S.H. coated steel in 1.0 M HCl solution.

Deposit	$-E_{\text{corr}}$ mV	β_a mV/decade	$-\beta_c$ mV/decade	i_{corr} $\mu\text{A}/\text{cm}^2$	% η
Uncoated steel	514.5	93.3	85.5	0.3915723	–
Steel + Ni-S.A	511.3	195.9	111.6	0.0302125	92.3
Steel + Ni-bio Cu-S.A	509.5	212.2	181.9	0.0157012	96.0

**Fig. 8.** a) Nyquist, b) Bode, and c) Phase angle plots of uncoated steel, and S.H. coated steel.

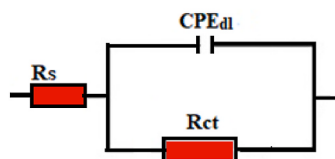


Fig. 9. The equivalent circuit model.

$$\% \eta = [(R_{ct} - R_{ct0}) / R_{ct}] \times 100 \quad (2)$$

Where R_{ct} and R_{ct0} represent the charge transfer resistance of S.H. coated steel and uncoated steel, respectively. The obtained EIS parameters are listed in Table 3. It is evident that both R_{ct} and $\% \eta$ values follow the trend: uncoated steel < steel + Ni-S.A < steel + Ni-bio Cu-S.A. The corrosion resistance of the S.H. coated steel using Ni-bio Cu-S.A surpasses several previously reported values [45–47]. The application of S.H. coatings to the steel results in an elevation of R_s , signaling greater solution resistance compared to the uncoated steel. The reduction in CPE for the S.H. coated steel signifies a significant decrease in adsorbed corrosive species to the steel surface, indicating improved protection efficiency for the S.H. coated steel. Moreover, the corrosion resistance of the S.H. coated steel with Ni-bio Cu-S.A is greater than that of steel coated with Ni-S.A. This can be attributed to the fact that bio Cu enhances superhydrophobicity. This slows down the corrosion process and enhances the overall corrosion resistance of the coating.

3.6. Mechanism of corrosion resistance performance

Bare steel surfaces possess a propensity to adsorb water molecules, rendering them susceptible to corrosion. The presence of chloride ions on uncoated steel surfaces further exacerbates the corrosion vulnerability. In contrast, steel coated with S.H. films introduces a protective paradigm. The micro- and nanostructures of the S.H. coating, enveloped in a hydrophobic material, contribute to its unique corrosion resistance. The intricate morphology of the S.H. coated steel, with its peaks and valleys, facilitates the entrapment of air within the valleys. The hydrophobic nature of the coating ensures that these air-filled interstices persist, creating a passivation barrier between the steel substrate and the corrosive environment. This air barrier becomes a pivotal element in impeding the progression of corrosion.

The obstructive effect of the trapped air plays a crucial role in diminishing the impact of aggressive ion species, notably chloride ions, prevalent in corrosive environments. The hindrance created by the entrapped air limits the direct interaction of these corrosive ions with the underlying steel surface. As a result, the superhydrophobic coating acts as a formidable defense mechanism, reducing the likelihood of aggressive ion attacks and mitigating corrosion [48–50].

4. Conclusion

In this study, an eco-friendly approach for the construction of two types of superhydrophobic (S.H.) coatings, Ni-S.A and Ni-bio Cu-S.A, was developed. The WCA of steel coated with Ni-S.A and Ni-bio Cu-S.A are $158^\circ \pm 0.9^\circ$, and $162^\circ \pm 1.1^\circ$, respectively.

The chemical stability results obtained in this study reveal that the Ni-S.A coating maintains its S.H. characteristics in a pH range of 3–11. On the other hand, the Ni-bio Cu-S.A coating demonstrates excellent chemical stability, retaining its S.H. characteristics even in a broader pH range of 1–13. This indicates the robust chemical resistance of these coatings against acidic and alkaline environments. In terms of mechanical stability, the Ni-S.A coating exhibits remarkable durability, maintaining its S.H. properties even after an abrasion length of 1100 mm. While, the Ni-bio Cu-S.A coating displays exceptional mechanical stability, retaining its S.H. characteristics till an abrasion length of 1900 mm. These findings highlight the strong mechanical integrity and resistance to physical wear of the S.H. coatings.

The corrosion behavior and protective properties of S.H. coatings on steel were thoroughly investigated. The corrosion resistance of the coated steel samples was evaluated using potentiodynamic polarization (PDP) and electrochemical impedance spectroscopy (EIS) techniques. The PDP results revealed that both Ni-S.A and Ni-bio Cu-S.A coatings effectively reduced the corrosion Current density (i_{corr}) compared to uncoated steel, indicating improved corrosion resistance. The EIS analysis provided valuable insights into the charge transfer resistance (R_{ct}) and impedance parameters of the coated steel samples. The results showed that the charge transfer resistance of the Ni-S.A coated steel was higher than that of uncoated steel, indicating enhanced corrosion resistance. Notably, the Ni-bio Cu-S.A-coated steel exhibited the highest R_{ct} value, indicating the most effective barrier against corrosive species. This can be attributed to the presence of bio Cu, which enhanced the superhydrophobicity and formed a protective barrier against corrosive agents.

Funding

"This research was funded by Princess Nourah bint Abdulrahman University Researchers Supporting project number (PNURSP2024R316), Princess Nourah bint Abdulrahman University, Riyadh, Saudi Arabia."

Table 3

The EIS parameters for the uncoated and S.H. coated steel in 1.0 M HCl solution.

Coat	R_s (Ohm.cm ²)	n_1	CPE $\times 10^{-6}$ (s ⁿ Ω^{-1} cm ²)	R_{ct} (Ohm.cm ²)	% η
Uncoated steel	0.2	0.78	53.4	12.1	–
Steel + Ni-S.A	1.1	0.76	36.2	234.2	94.8
Steel + Ni-bio Cu-S.A	1.4	0.72	25.2	439.5	97.2

Data availability statement

"All data in this study will be available on request."

CRedit authorship contribution statement

R.S. Almfarij: Writing – original draft, Funding acquisition, Formal analysis, Conceptualization. **M. Saadawy:** Writing – original draft, Methodology, Investigation, Data curation, Conceptualization. **M.E. Mohamed:** Writing – review & editing, Writing – original draft, Visualization, Validation, Supervision, Project administration, Methodology, Investigation, Funding acquisition, Formal analysis, Data curation, Conceptualization.

Declaration of competing interest

The authors declare the following financial interests/personal relationships which may be considered as potential competing interests: This research was supported by Princess Nourah bint Abdulrahman University Researchers Supporting project number (PNURSP2024R316), Princess Nourah bint Abdulrahman University, Riyadh, Saudi Arabia."

Acknowledgments

"The authors would like to thank Princess Nourah bint Abdulrahman University Researchers Supporting project number (PNURSP2024R316), Princess Nourah bint Abdulrahman University, Riyadh, Saudi Arabia."

References

- [1] C. Su, X. Huang, L. Zhang, Y. Zhang, Z. Yu, C. Chen, Y. Ye, S. Guo, Robust superhydrophobic wearable piezoelectric nanogenerators for self-powered body motion sensors, *Nano Energy* 107 (2023) 108095, <https://doi.org/10.1016/j.nanoen.2022.108095>.
- [2] X. Huang, M. Sun, X. Shi, J. Shao, M. Jin, W. Liu, R. Zhang, S. Huang, Y. Ye, Chemical vapor deposition of transparent superhydrophobic anti-icing coatings with tailored polymer nanoarray architecture, *Chem. Eng. J.* 454 (2023) 139981, <https://doi.org/10.1016/j.cej.2022.139981>.
- [3] F. Sahin, N. Celik, A. Ceylan, S. Pekdemir, M. Ruzi, M.S. Onses, Antifouling superhydrophobic surfaces with bactericidal and SERS activity, *Chem. Eng. J.* 431 (2022) 133445, <https://doi.org/10.1016/j.cej.2021.133445>.
- [4] L. Jiang, H. Zheng, J. Xiong, Z. Fan, T. Shen, H. Xie, M. Chen, J. Li, Z. Gu, H. Li, W. Li, Fabrication of negative carbon superhydrophobic self-cleaning concrete coating: high added-value utilization of recycled powders, *Cem. Concr. Compos.* 136 (2023) 104882, <https://doi.org/10.1016/j.cemconcomp.2022.104882>.
- [5] J. Zhao, R. Sun, C. Liu, J. Mo, Application of ZnO/epoxy resin superhydrophobic coating for buoyancy enhancement and drag reduction, *Colloids Surfaces A Physicochem. Eng. Asp.* 651 (2022) 129714, <https://doi.org/10.1016/j.colsurfa.2022.129714>.
- [6] R.S. Almfarij, H.A. Fetouh El Sayed, M.E. Mohamed, Eco-friendly approach for the construction of superhydrophobic coating on stainless steel metal based on biological metal-organic framework and its corrosion resistance performance, *Materials* 16 (2023) 4728, <https://doi.org/10.3390/ma16134728>.
- [7] M.E. Mohamed, B.A. Abd-El-Nabey, Fabrication of a biological metal-organic framework based superhydrophobic textile fabric for efficient oil/water separation, *Sci. Rep.* 12 (2022) 15483, <https://doi.org/10.1038/s41598-022-19816-y>.
- [8] Z. Wu, C. Shi, A. Chen, Y. Li, S. Chen, D. Sun, C. Wang, Z. Liu, Q. Wang, J. Huang, Y. Yue, S. Zhang, Z. Liu, Y. Xu, J. Su, Y. Zhou, S. Wen, C. Yan, Y. Shi, X. Deng, L. Jiang, B. Su, Large-scale, abrasion-resistant, and Solvent-free superhydrophobic objects fabricated by a selective laser sintering 3D printing strategy, *Adv. Sci.* 10 (2023) 1–7, <https://doi.org/10.1002/advs.202207183>.
- [9] S. Zhu, W. Deng, Y. Su, Recent advances in preparation of metallic superhydrophobic surface by chemical etching and its applications, *Chinese J. Chem. Eng.* (2023), <https://doi.org/10.1016/j.cjche.2023.02.018>.
- [10] Z. Wang, Y. Shen, J. Tao, S. Liu, J. Jiang, Y. Xu, W. Liu, H. Li, An integrated superhydrophobic anti/de-icing film heater with low energy consumption: interpenetration behavior of components based on wet-film spraying method, *Appl. Therm. Eng.* 223 (2023) 120028, <https://doi.org/10.1016/j.applthermaleng.2023.120028>.
- [11] N. Gao, G. Ding, C. Wang, F. Chen, Y. Wang, H. Ma, A facile strategy to fabricate bionic superhydrophobic armor based on utilization of metallographic structure heredity and reconstruction of anodized oxide film on alloy, *Surface. Interfac.* 34 (2022) 102351, <https://doi.org/10.1016/j.surfin.2022.102351>.
- [12] F. Wang, R. Ma, Y. Tian, Fabrication of superhydrophobic/oleophilic starch cryogel via a simple sol-gel immersion process for removing oil from water, *Ind. Crops Prod.* 184 (2022) 115010, <https://doi.org/10.1016/j.indcrop.2022.115010>.
- [13] M. Cui, J. Wu, J. Wei, Z. Wei, Near-infrared photodynamic antibacterial enhanced superhydrophobic electrospun membrane surfaces, *Surf. Coating. Technol.* 463 (2023) 129497, <https://doi.org/10.1016/j.surfcoat.2023.129497>.
- [14] M.E. Mohamed, O. Adel, E. Khamis, Fabrication of biochar-based superhydrophobic coating on steel substrate and its UV resistance, anti-scaling, and corrosion resistance performance, *Sci. Rep.* 13 (2023) 9453, <https://doi.org/10.1038/s41598-023-36589-0>.
- [15] M.E. Mohamed, P.S. Mekhaieel, F.M. Mahgoub, Construction of superhydrophobic graphene-based coating on steel substrate and its ultraviolet durability and corrosion resistance properties, *Sci. Rep.* 13 (2023).
- [16] E. Velayi, R. Norouzbegi, Fabrication of epoxy/SiO₂/ZnO superhydrophobic nanocomposite mesh membranes for oil-water separation: correlating oil flux to fabrication parameters via Box-Behnken design, *Appl. Surf. Sci.* 611 (2023) 155594, <https://doi.org/10.1016/j.apsusc.2022.155594>.
- [17] M. Yu, L. Yang, L. Yan, T. Wang, Y. Wang, Y. Qin, L. Xiong, R. Shi, Q. Sun, ZnO nanoparticles coated and stearic acid modified superhydrophobic chitosan film for self-cleaning and oil-water separation, *Int. J. Biol. Macromol.* 231 (2023) 123293, <https://doi.org/10.1016/j.ijbiomac.2023.123293>.

- [18] J. Yang, T. He, X. Li, R. Wang, S. Wang, Y. Zhao, H. Wang, Rapid dipping preparation of superhydrophobic TiO₂ cotton fabric for multifunctional highly efficient oil-water separation and photocatalytic degradation, *Colloids Surfaces A Physicochem. Eng. Asp.* 657 (2023) 130590, <https://doi.org/10.1016/j.colsurfa.2022.130590>.
- [19] F. Khan, A. Shahid, H. Zhu, N. Wang, M.R. Javed, N. Ahmad, J. Xu, M.A. Alam, M.A. Mehmood, Prospects of algae-based green synthesis of nanoparticles for environmental applications, *Chemosphere* 293 (2022) 133571, <https://doi.org/10.1016/j.chemosphere.2022.133571>.
- [20] V. Nayak, K.R. Singh, R. Verma, M.D. Pandey, J. Singh, R. Pratap Singh, Recent advancements of biogenic iron nanoparticles in cancer theranostics, *Mater. Lett.* 313 (2022) 131769, <https://doi.org/10.1016/j.matlet.2022.131769>.
- [21] B.A. Omran, K.H. Baek, Control of phytopathogens using sustainable biogenic nanomaterials: recent perspectives, ecological safety, and challenging gaps, *J. Clean. Prod.* 372 (2022) 133729, <https://doi.org/10.1016/j.jclepro.2022.133729>.
- [22] I.I. Alao, I.P. Oyekunle, K.O. Iwuozor, E.C. Emenike, Green synthesis of copper nanoparticles and investigation of its antimicrobial properties, *Adv. J. Chem. B Nat. Prod. Med. Chem.* 4 (2022) 39–52, <https://doi.org/10.22034/ajcb.2022.323779.1106>.
- [23] V.W. Xu, M.Z.I. Nizami, I.X. Yin, O.Y. Yu, C.Y.K. Lung, C.H. Chu, Application of copper nanoparticles in dentistry, *Nanomaterials* 12 (2022) 805, <https://doi.org/10.3390/nano12050805>.
- [24] R.V. Bordiwala, Green synthesis and applications of metal nanoparticles. - A review article, *Results Chem* 5 (2023) 100832, <https://doi.org/10.1016/j.rechem.2023.100832>.
- [25] B.A. Abd-El-Nabey, M. Ashour, A.M. Aly, M.E. Mohamed, Fabrication of robust superhydrophobic nickel films on steel surface with high corrosion resistance, mechanical and chemical stability, *J. Eng. Mater. Technol.* 144 (2022), <https://doi.org/10.1115/1.4052768/1122255>.
- [26] M.E. Mohamed, B.A. Abd-El-Nabey, Corrosion performance of a steel surface modified by a robust graphene-based superhydrophobic film with hierarchical roughness, *J. Mater. Sci.* (2022), <https://doi.org/10.1007/s10853-022-07325-2>.
- [27] S.V. nedenkov, S. A. A.D. Nomerovskii, A.K. Tsvetnikov, S.L. Sinebryukhov, Gnedkov, Cold-sprayed composite metal-fluoropolymer coatings for alloy protection against corrosion and wear, *Materials* 16 (2023) 918.
- [28] T. Zehra, M. Kaseem, Recent advances in surface modification of plasma electrolytic oxidation coatings treated by non-biodegradable polymers, *J. Mol. Liq.* 365 (2022) 120091, <https://doi.org/10.1016/j.molliq.2022.120091>.
- [29] M. Kaseem, H. Choe, Triggering the hydroxyapatite deposition on the surface of PEO-coated Ti e 6Al e 4V alloy via the dual incorporation of Zn and Mg ions, *J. Alloys Compd.* 819 (2020) 153038, <https://doi.org/10.1016/j.jallcom.2019.153038>.
- [30] A.S. Gnedkov, S.L. Sinebryukhov, A.D. Nomerovskii, V.S. Filonina, A.Y. Ustinov, S. V Gnedkov, Design of self-healing PEO-based protective layers containing in-situ grown LDH loaded with inhibitor on the MA8 magnesium alloy, *J. Magnesium Alloys* (2023), <https://doi.org/10.1016/j.jma.2023.07.016>.
- [31] A.S. Gnedkov, S.L. Sinebryukhov, V.S. Filonina, N.G. Plekhova, S. V Gnedkov, Smart composite antibacterial coatings with active corrosion protection of magnesium alloys, *J. Magnes. Alloy.* 10 (2022) 3589–3611, <https://doi.org/10.1016/j.jma.2022.05.002>.
- [32] A.S. Gnedkov, V.S. Filonina, S.L. Sinebryukhov, S. V Gnedkov, A superior corrosion protection of Mg alloy via smart nontoxic hybrid inhibitor-containing coatings, *Molecules* 28 (2023) 2538.
- [33] S.V. Gnedkov, S. A. S.L. Sinebryukhov, V.S. Filonina, A.Y. Ustinov, S.V. Sukhovkhor, Gnedkov, New polycaprolactone-containing self-healing coating design for enhance corrosion resistance of the magnesium and its alloys, *Polymers* 15 (2023) 202.
- [34] A. Fattah-alhosseini, R. Chaharmahali, K. Babaei, M. Nouri, A review of effective strides in amelioration of the biocompatibility of PEO coatings on Mg alloys, *J. Magnes. Alloy.* 10 (2022) 2354–2383, <https://doi.org/10.1016/j.jma.2022.09.002>.
- [35] D.M. Ragheb, A.M. Abdel-Gaber, F.M. Mahgoub, M.E. Mohamed, Eco-friendly method for construction of superhydrophobic graphene-based coating on copper substrate and its corrosion resistance performance, *Sci. Rep.* 12 (2022) 1–14, <https://doi.org/10.1038/s41598-022-22915-5>.
- [36] C. Du, X. He, F. Tian, X. Bai, C. Yuan, Preparation of superhydrophobic steel surfaces with chemical stability and corrosion, *Coatings* 9 (2019) 1–10.
- [37] L. Ma, J. Wang, Z. Zhang, Y. Kang, M. Sun, L. Ma, Preparation of a superhydrophobic TiN/PDTE composite film toward self-cleaning and corrosion protection applications, *J. Mater. Sci.* 56 (2021) 1413–1425, <https://doi.org/10.1007/s10853-020-05364-1>.
- [38] P. Zhu, L. Zhu, F. Ge, G. Wang, Z. Zeng, Sprayable superhydrophobic coating with high mechanical/chemical robustness and anti-corrosion, *Surf. Coating. Technol.* 443 (2022) 128609, <https://doi.org/10.1016/j.surfcoat.2022.128609>.
- [39] D. Nanda, A. Sahoo, A. Kumar, B. Bhushan, Facile approach to develop durable and reusable superhydrophobic/superoleophilic coatings for steel mesh surfaces, *J. Colloid Interface Sci.* 535 (2019) 50–57, <https://doi.org/10.1016/j.jcis.2018.09.088>.
- [40] M.E. Mohamed, A. Ezzat, A.M.A. Gaber, Fabrication of eco - friendly graphene - based superhydrophobic coating on steel substrate and its corrosion resistance, chemical and mechanical stability, *Sci. Rep.* 12 (2022) 1–15, <https://doi.org/10.1038/s41598-022-14353-0>.
- [41] F. Paquin, J. Rivnay, A. Salleo, N. Stingelin, C. Silva, Multi-phase semicrystalline microstructures drive exciton dissociation in neat plastic semiconductors, *J. Mater. Chem. C* 3 (2015) 10715–10722, <https://doi.org/10.1039/b000000x>.
- [42] L. Li, X. Li, J. Chen, L. Liu, J. Lei, N. Li, G. Liu, F. Pan, One-step spraying method to construct superhydrophobic magnesium surface with extraordinary robustness and multi-functions, *J. Magnes. Alloy.* 9 (2021) 668–675, <https://doi.org/10.1016/j.jma.2020.06.017>.
- [43] A.S. Gnedkov, S.L. Sinebryukhov, V.S. Filonina, S. V Gnedkov, Hydroxyapatite-containing PEO-coating design for biodegradable Mg-0 . 8Ca alloy : formation and corrosion behaviour, *J. Magnesium Alloys* (2022), <https://doi.org/10.1016/j.jma.2022.12.002>.
- [44] M. Kaseem, T. Zehra, T. Hussain, Y. Gun, Electrochemical response of MgO/Co 3 O 4 oxide layers produced by plasma electrolytic oxidation and post treatment using cobalt nitrate, *J. Magnes. Alloy.* 11 (2023) 1057–1073, <https://doi.org/10.1016/j.jma.2022.08.008>.
- [45] J.e. Qu, C. Yu, C. Nie, H. Wang, Z. Cao, Y. Li, X. Wang, A new environmentally friendly approach to prepare superhydrophobic colored stainless steel surface for decoration, anti-corrosion and self-cleaning, *J. Mater. Sci.* 56 (2021) 854–869, <https://doi.org/10.1007/s10853-020-05293-z>.
- [46] X. sen Lv, Y. Qin, H. Liang, B. Zhao, Y. He, X. Cui, A facile method for constructing a superhydrophobic zinc coating on a steel surface with anti-corrosion and drag-reduction properties, *Appl. Surf. Sci.* 562 (2021) 150192, <https://doi.org/10.1016/j.apsusc.2021.150192>.
- [47] P. Varshney, S.S. Mohapatra, A. Kumar, Durable and regenerable superhydrophobic coating on steel surface for corrosion protection, *J. Bio- Tribo-Corrosion.* 7 (2021) 1–11, <https://doi.org/10.1007/s40735-021-00518-3>.
- [48] J. Ou, X. Chen, Corrosion resistance of phytic acid/Ce (III) nanocomposite coating with superhydrophobicity on magnesium, *J. Alloys Compd.* 787 (2019) 145–151, <https://doi.org/10.1016/j.jallcom.2019.02.003>.
- [49] G. Barati Darband, M. Aliofkhaezei, S. Khorsand, S. Sokhanvar, A. Kaboli, Science and engineering of superhydrophobic surfaces: review of corrosion resistance, chemical and mechanical stability, *Arab. J. Chem.* 13 (2020) 1763–1802, <https://doi.org/10.1016/j.arabjc.2018.01.013>.
- [50] T.P. Rasitha, S.C. Vanithakumari, R.P. George, J. Philip, Template-free one-step electrodeposition method for fabrication of robust superhydrophobic coating on ferritic steel with self-cleaning ability and superior corrosion resistance, *Langmuir* 35 (2019) 12665–12679, <https://doi.org/10.1021/acs.langmuir.9b02045>.